Aluminum Scandium Nitride for mm-Wave Acoustic Filtering: Challenges and Outlook

Azadeh Ansari
School of Electrical and Computer Engineering,
Georgia Institute of Technology, Atlanta, GA, USA
azadeh.ansari@ece.gatech.edu

In the recent years, microwave and millimeter wave frequencies have been untapped by acoustic devices for frontend filtering applications. Acoustic filtering promises low power consumption, linearity, small footprint and low insertion loss. Thus, many research and industry groups have been working on extending the frequencies of bulk acoustic wave (BAW) and surface acoustic wave (SAW) devices beyond 6 GHz, to accommodate the fast-growing cellphone and new radio wireless bands. Such frequency scaling is made possible thanks to the advances in the resonator material quality. Aluminum Scandium Nitride, amongst other piezoelectric materials, has been an attractive candidate for microwave acoustic filtering due to i) enhanced piezoelectricity at high Sc contents compared to pure AlN, and ii) thin film deposition/growth versatility and compatibility with CMOS or III-V fabrication processes.

This work first reviews some of the recent advances in AlScN material growth, as well as resonator device innovations, that have led to the realization of high-performance filters with frequencies above 12 GHz and up to 50 GHz. The reported $Al_{1-x}Sc_xN$ resonator figures of merit such as Q, k_t^2, and power handling are summarized, followed by a discussion of these metric vs Sc concentration. Finally, various types of phonon scattering mechanisms present in $Al_{1-x}Sc_xN$ thin films will be discussed that give rise to a lower Q and lower thermal conductivity with increasing x (=Sc/(Al+Sc)). Specifically, phonon scattering from alloys and grain boundaries are shown to impact $Al_{1-x}Sc_xN$ Q compared to AlN Q. Despite the great promise in achieving wide bandwidth filters, the lower Q and thermal conductivity in Al1-xScxN need to be considered and accounted for in the design of high-performance filters.

***Summary*— This work summarizes the recent advances in AlScN acoustic resonators towards mm-wave acoustic filtering applications. The phonon scattering mechanisms and microstructure properties that give rise to filter metrics will be outlined.**

Keywords*— *Acoustic; BAW; phonon; quality factor; Aluminum Nitride; mm wave; coupling; thermal conductivity; filtering

I. Introduction

Aluminum scandium nitride ($Al_{1-x}Sc_xN$) has been a promising piezoelectric material for modern wide-band high-frequency acoustic filters, with the prospect of untapping millimeter wave frequencies. Introducing Sc to aluminum nitride (AlN) can boost the piezoelectric coefficient d_{33} up to five times than that of pure AlN, which translates to enhanced effective electromechanical coupling coefficients (k_{eff}^2), and wider bandwidth filters [1]. Recent research has been focused on the growth/deposition of high quality $Al_{1-x}Sc_xN$ films with submicron thickness for 5G applications. Furthermore, the discovery of ferroelectric properties in $Al_{1-x}Sc_xN$ with x> 20% [3] has opened up new research thrusts similar to work done with BST [8], using the integration of high-Q tunable capacitors and acoustic resonators to build filters with larger bandwidths than the traditional fractional bandwidths limited to 0.5 k_t^2, with larger tuning capability.

II. Methods/Results

To target frequencies above 6 GHz, piezoelectric films should be thinned down to submicron scales, when targeting the fundamental thickness resonance mode, which yields the highest achievable k_t^2. This usually challenges the crystalline microstructure, particularly, when Si is used as the host substrate. Epitaxial methods (*e.g.* MOCVD, MBE) have been recently used to improve the crystal quality of ultrathin $Al_{1-x}Sc_xN$. However, the metal electrodes should be scaled down with the piezo thickness to ensure high electromechanical coupling, without limiting the electrical Q due to high sheet resistivity. Our group uses MBE-grown AlScN films with MBE-grown epitaxial metal layers on a Si substrate. The fundamental thickness-resonance mode peaks at 18.6 GHz with a Bode Q_{max} of 130 and k_t^2 of 14.5%, the highest reported k_t^2 to date for 16-20 GHz FBARs. Figure 1 shows the COMSOL simulation results of FBAR k_t^2 vs. electrode/piezo-film thickness ratio, indicating the optimum normalized thickness range for achieving high k_t^2 around 0.2~0.3. While thinned down electrodes (< 50 nm) help achieve high k_t^2, the sheet resistivity will increase particularly when sputtered. Fig. 2 shows that epitaxial Mo films with 50 nm thickness can show sheet resistivity values as high as the bulk material, while sputtered Mo shows significantly higher sheet resistivity. This justifies the use of epitaxial metal electrodes for 16-20 GHz FBARs.

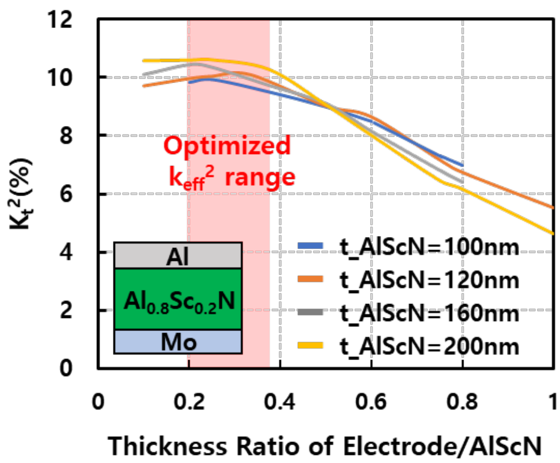

Fig. 1: Finite Element Analysis simulations of k_t^2 based on the thickness ratio between the electrode/$Al_{0.8}Sc_{0.2}N$ thickness ratio. The $Al_{0.8}Sc_{0.2}N$ thickness is also swept and k_t^2 is plotted. This plot shows that the metal layers should be scaled with the piezoelectric thickness to preserve a high k_t^2.

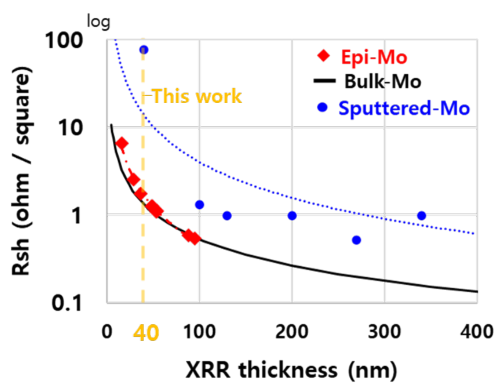

Fig. 2. Measured and fitted sheet resistivity (Rsh) vs. thickness of epitaxially grown Mo, sputter-deposited Mo, and bulk Mo [6].

III. DISCUSSION/INTERPRETATION

3.1. $Al_{1-x}Sc_xN$ Resonator Metric Trends

Optimizing the metal growth and thickness can help achieve k_t^2 values close to the piezoelectric material coupling coefficients. Furthermore, increasing the Sc content (x in $Al_{1-x}Sc_xN$) increases the piezoelectric material coupling. Fig. 3 (a,b) shows a collection of the reported k_t^2 and Q factor for $Al_{1-x}Sc_xN$ resonators vs. x [1]. This indicates that while the resonator k_t^2 increases with increasing x, the resonator Q drops as x increases. From the presented literature review increasing the Sc content in $Al_{1-x}Sc_xN$ alloy severely impacts the resonator quality factor. This can be attributed to degraded crystal quality (*e.g.* increased boundary scattering), as well as increased alloy scattering. Controlled experiments with varying only one material parameter should be conducted to shed light on the dependency of Q on $Al_{1-x}Sc_xN$ alloys with different crystalline properties. Fig. 3(c) shows the measured and modeled thermal conductivity of $Al_{1-x}Sc_xN$ vs. x, showing a 30x drop at x=30% compared to pure AlN. This indicates lower phonon lifetimes and increased phonon scattering [1]. The lower thermal conductivity values for high Sc% alloys impose challenges on the power handling of $Al_{1-x}Sc_xN$ resonators that should be accounted for in the resonator design [7].

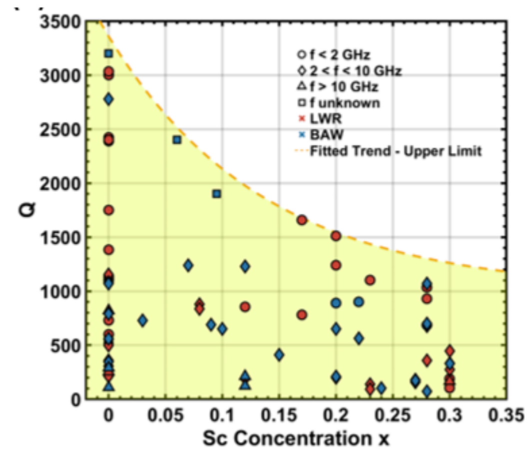

(a)

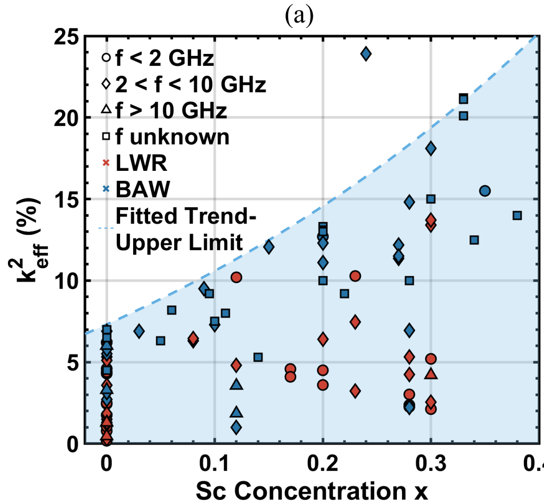

(b)

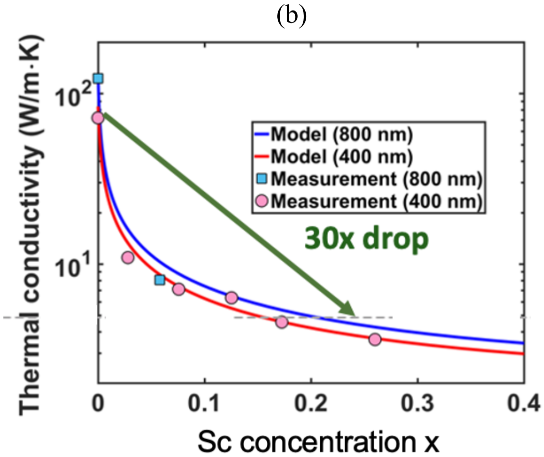

(c)

Fig. 3. Summary of reported metrics of $Al_{1-x}Sc_xN$ resonator in the last decade from multiple research and industry groups: (a) Q vs. x [1], (b) k_t^2 trends vs. x [1], (c) thermal conductivity trends vs. x (measured and modelled) [5].These figures indicate that while k_t^2 improves with increasing x, the drop in Q and thermal conductivity can impose challenges in the resonator operation [7].

3.2. High- k_t^2 $Al_{1-x}Sc_xN$ FBARs

In this section, the highest k_t^2 AlScN FBARs to date are presented from our research group. Fig. 4 shows the fabricated FBAR SEM images and measured responses in our group using (i) a 1um $Al_{0.7}Sc_{0.3}N$ film targeted for 3 GHz with a record high k_t^2 of 19% [3]; and (ii) a 120 nm $Al_{0.8}Sc_{0.2}N$ film operating at 18 GHz with a k_t^2 of 15%. In both cases the top metal electrodes were grown/deposited in the same run as the AlScN deposition/growth to avoid surface oxidation of AlScN.

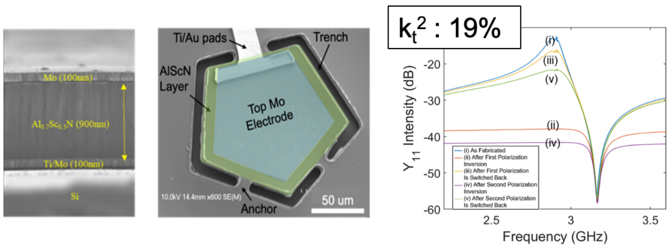

(a) (b) (c)

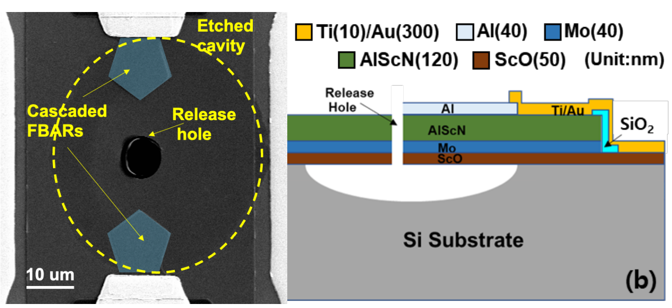

(d) (e)

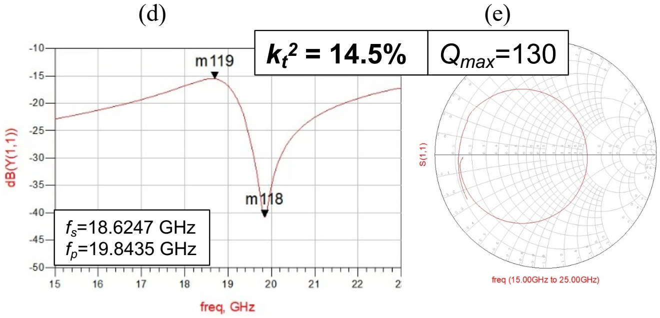

(f)

Fig. 4. SEM images and measured responses of a 3 GHz and 18.6 GHz FBAR, based on 30% and 20% AlScN, respectively. (a) Cross section SEM, (b) FBAR SEM, (c) admittance frequency response, showing a k_t^2 of 19%. (d) SEM image of an all-epitaxial cascaded FBAR with epi-metals. (e) cross sections schematic of an 18 GHz FBAR with frontside release. (f) Y11 frequency response and the raw data Q circle showing a record high k_t^2 of 14.5%.

3.3. Phonon Scattering Dependence on $Al_{1-x}Sc_xN$ Crystal Microstructure

Here, we theoretically analyze the the major phonon scattering mechanisms present in $Al_{1-x}Sc_xN$ lattice (Fig. 5). The results suggest that while both AlN and $Al_{1-x}Sc_xN$ phonon lifetimes can be limited by microstructure-dependent grain boundary scattering, $Al_{0.7}Sc_{0.3}N$ suffers from a decrease of phonon lifetime by up to four orders of magnitude due to alloy scattering, attributing to the lower *Q* compared to AlN acoustic resonators.

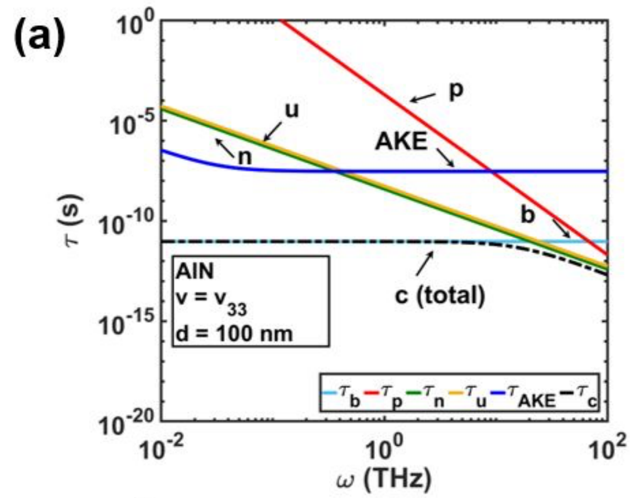

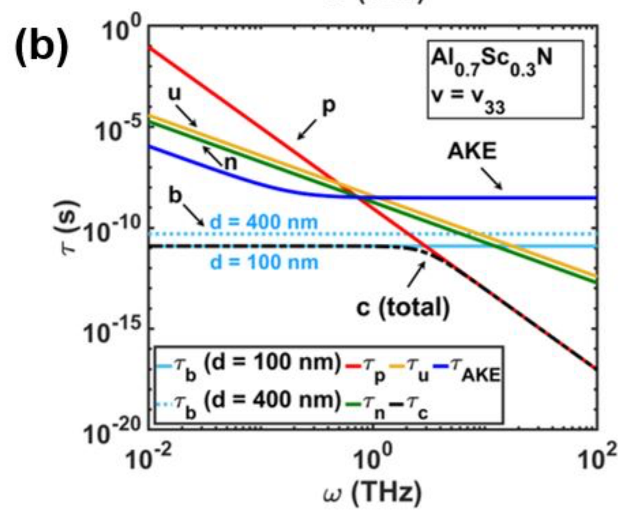

Fig. 5. Phonon lifetime compositions at room temperature (292K) of (a) AlN compared with (b) $Al_{0.7}Sc_{0.3}N$. Even for the same grain boundary size (d = 100 nm), alloy scattering degrades the lifetime of high-frequency phonons for $Al_{0.7}Sc_{0.3}N$. Estimation of τ_b with d = 400 nm is plotted on (b) as a comparison. [1]

Fig. 6 shows evidence of nonidealities in the crystallinity of AlN and AlScN films when sputtered and grown by MBE. The in-plane grain boundary size for the sputtered sample ranges from 23-50 nm [4]. While, the in-plane grain boundary size for the MBE-grown films range from 150-750 nm [4]. Both sputtered and MBE grown AlN films show columnar c-axis growth with larger cross-plane grain boundary sizes compared to the in-plane grain boundary size. All crystalline nonidealities, such as small in-plane grain boundary sizes, surface roughness defects and abnormally-oriented grains should be taken into account when projecting the ultimate Q of acoustic resonators based on $Al_{1-x}Sc_xN$, because they increase the phonon scattering life time.

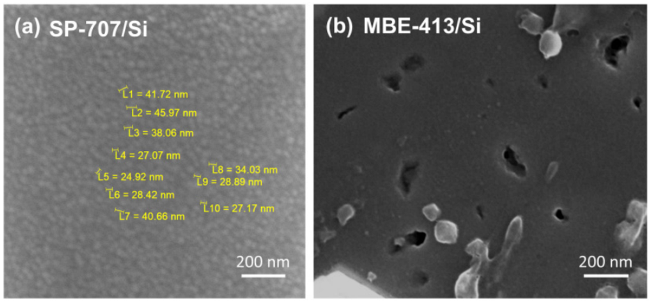

Top SEM images: (a) sputtered AlN, and (b) MBE-grown AlN on Si.

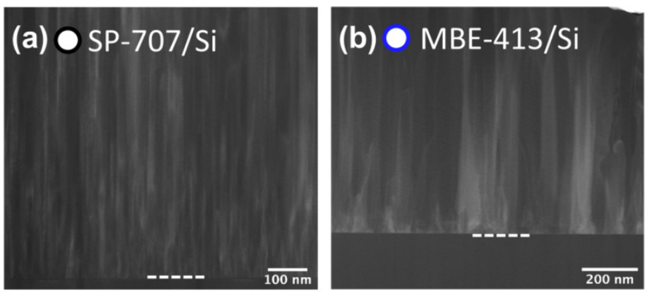

Cross-sectional SEM images: (a) sputtered AlN, and (b) MBE-grown AlN on Si.

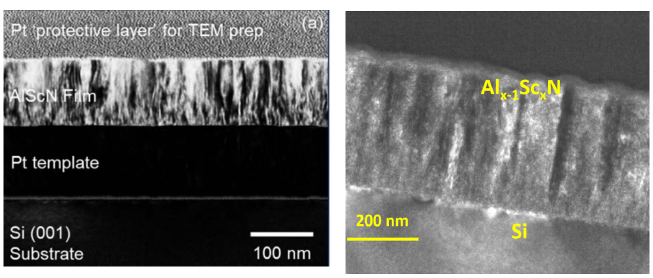

Cross-sectional SEM images of AlScN films sputtered and MBE-grown on Si. [5, 10]

Fig. 6. Evidence of limited crystallinity in sputtered- and MBE-grown AlN and $Al_{1-x}Sc_xN$ thin films. The smaller grain boundary sizes should be taken into account when estimating the quality factor of the resonator. The grain boundaries also impact the surface roughness that can impact the Q significantly.

IV. Conclusions

This invited paper outlined some of the challenges in scaling acoustic resonators for mm-wave filtering application. Epitaxially-grown thin metal films and AlScN films were presented as viable candidates that preserve crystalline quality and sheet conductance for the electrodes. The resonator metric trends (*i.e.* Q, k_t^2, *thermal conductivity)* were studied as the Sc content (x) increases in $Al_{1-x}Sc_xN$, indicating the benefits and challenges of using $Al_{1-x}Sc_xN$ as the material platform. Some of the results of our group that set record high k_t^2 were presented, showing a k_t^2 of ~15% at 18.6 GHz epi-FBAR. Finally, phonon scattering time for various scattering mechanisms were analytically calculated. It was observed that alloy scattering in particular, degrades high frequency phonon life times and is higher for $Al_{1-x}Sc_xN$ with higher x.

Acknowledgement

The author would like to acknowledge Prof. Zetian Mi and his team at the University of Michigan for MBE growth of AlScN; IQE for preparing epitaxial Mo samples, and Dr. Mingyo Park, Yue Zheng, and Jialin Wang for the resonator fabrication and characterization. The devices were fabricated at Georgia Tech IEN clean room facilities. The author acknowledges DARPA COFFEE for funding and helpful discussions with Dr. Benjamin Griffin.

References

[1] Y. Zheng, M. Park, C. Yuan and A. Ansari, “Effect of Scandium Composition on the Phonon Scattering Lifetime of Aluminum Scandium Nitride Acoustic Wave Resonators,” *2023 IEEE 36th International Conference on Micro Electro Mechanical Systems (MEMS)*, Munich, Germany, 2023, pp. 1186-1189, doi: 10.1109/MEMS49605.2023.10052227.

[2] M. Akiyama, et al., “Enhancement of Piezoelectric Response in Scandium Aluminum Nitride Alloy Thin Films Prepared by Dual Reactive Cosputtering,” *Adv. Mater.*, vol. 21, no. 5, pp. 593–596, Feb. 2009. https://doi.org/10.1002/adma.200802611.

[3] J. Wang, M. Park, S. Mertin, T. Pensala, F. Ayazi and A. Ansari, “A Film Bulk Acoustic Resonator Based on Ferroelectric Aluminum Scandium Nitride Films,” *Journal of Microelectromechanical Systems*, vol. 29, no. 5, pp. 741-747, Oct. 2020, doi: 10.1109/JMEMS.2020.3014584.

[4] Y. Song, *et al.*, “Growth-microstructure-thermal property relations in AlN thin films,” *J. Appl. Phys.*, vol. 132, no. 17, p. 175108, Nov. 2022. https://doi.org/10.1063/5.0106916.

[5] C. Yuan et al., “Phonon heat conduction in $Al_{1-x}Sc_xN$ thin films,” *Materials Today Physics*, vol. 21, pp. 100498, Feb. 2021. https://doi.org/10.1016/j.mtphys.2021.100498.

[6] A. Clark et al., “Epitaxial materials for RF filters,” in CS MANTECH Digest , 2019, pp. 10–12.

[7] Y. Zheng, M. Park, A. Ansari, C. Yuan and S. Graham, “Self-Heating and Quality Factor: Thermal Challenges in Aluminum Scandium Nitride Bulk Acoustic Wave Resonators,” *2021 21st International Conference on Solid-State Sensors, Actuators and Microsystems (Transducers),* Orlando, FL, USA, 2021, pp. 321-324, doi: 10.1109/Transducers50396.2021.94956.

[8] S. Nam, D. Psychogiou and A. Mortazawi, "Reconfigurable Transfer Function BST Acoustic Wave Lumped Element Resonator Filters," 2021 51st European Microwave Conference (EuMC), London, United Kingdom, 2022, pp. 301-304, doi: 10.23919/EuMC50147.2022.9784219.

[9] M. Park, Z. Hao, R. Dargis, A. Clark and A. Ansari, "Epitaxial Aluminum Scandium Nitride Super High Frequency Acoustic Resonators," in Journal of Microelectromechanical Systems, vol. 29, no. 4, pp. 490-498, Aug. 2020, doi: 10.1109/JMEMS.2020.3001233.

[10] D. Wang et al., "Ferroelectric C-Axis Textured Aluminum Scandium Nitride Thin Films of 100 nm Thickness," 2020 Joint Conference of the IEEE International Frequency Control Symposium and International Symposium on Applications of Ferroelectrics (IFCS-ISAF), Keystone, CO, USA, 2020, pp. 1-4, doi: 10.1109/IFCS-ISAF41089.2020.9234910.